Discover Oncology

ANALYSIS Open Access

Integrated single-cell multi-omics analysis unveils heterogeneity in the prostate cancer tumor microenvironment

Zongwei Mei[1], Chen Chen[1], Jilong Zhou[1] and Qing Jiang[1*]

*Correspondence:
Qing Jiang
300899@hospital.cqmu.edu.cn
[1]Department of Urology, The Second Afliated Hospital of Chongqing Medical University, Chongqing 400010, People's Republic of China

Abstract

Background Prostate cancer (PCa) is a heterogeneous disease characterised by a highly complex cellular ecosystem within its tumour microenvironment (TME). However, the crosstalk patterns between tumour and immune cells remain poorly understood.

Methods Single cell RNA sequencing, spatial transcriptomics and bulk RNA-seq data were integrated to explore key Tregs cells modules and genes involved in PCa processes in the tumour microenvironment.

Results We found that the oxidative phosphorylation and apoptosis signaling pathways of Tregs cells in PCa patients is significantly activated. Tregs cells and Tumour cells may interact through PPIA-BSG ligand-receptor pairs to form an immunosuppressive microenvironment. Using high-dimensional weighted gene co-expression network analysis, we identified 6 key functional modules in Tregs from PCa. The spatial localization of these modules in tumor tissues was further validated using spatial transcriptomics data. Subsequent differential modules analysis revealed that the M2 module exhibited the most significant changes. A Cox proportional hazards model was then constructed based on this module, leading to the identification of 8 key prognostic genes, including ANKRD37, CHORDC1, DOK2, HSPA6, RGCC, SERPINH1, STIP1, and UBB. These genes hold promise as potential molecular markers for the diagnosis and prognostic evaluation of PCa.

Conclusion These findings reveal potential ligand-receptor interactions in the tumour microenvironment of PCa patients and key Tregs cell module genes involved in the formation of an immunosuppressive microenvironment. Targeting these cells and genes will help advance the treatment of PCa.

Keywords Prostate cancer, Tumour microenvironment, Single-cell multi omics, Tregs cells, Tumour immunity

1 Introduction

Prostate cancer (PCa) is the most common malignant tumour in men worldwide and is composed of a mixture of tumour and non-tumour cell types [1–3]. The development of prostate tissue cancer involves complex interactions between tumour cells and

surrounding immune cells [4, 5]. Recruitment/activation of tumour-infiltrating regulatory T cells can impair antigen recognition, leading to reduced cytotoxic function or proliferation of CD8 + T cells [6–8]. These studies suggest that elucidating the potential crosstalk mechanisms of tumour immune microenvironment cells will aid in the treatment of PCa.

On the other hand, regulatory T (Treg) cells are an important component of immunosuppressive TME [9, 10]. Previous studies have shown that an increase in the frequency of Tregs within tumors is associated with poor prognosis in patients with various types of cancer [11–13]. The heterogeneity and plasticity of Tregs within tumors increase the complexity of their roles in tumors immunity and immunotherapy responses [14]. Recent studies have shown that the hypoxic state in the solid tumor microenvironment promotes the metabolic advantage of Treg dependent oxidative phosphorylation, further enhancing its immunosuppressive function [15]. However, the heterogeneity of Tregs and their potential molecular driving factors in the PCa tumor microenvironment have not been fully elucidated.Here, we integrated single-cell and spatial transcriptomic analysis to investigate the cellular interaction status in the PCa tumor microenvironment. We identified key ligand receptor pairs involved in immune suppression in the tumor microenvironment and their significant spatial co-localisation. In addition, we used high-dimensional weighted gene co-expression network analysis to identify multiple Tregs cell modules and employed Cox proportional hazards model to determine key prognostic genes.

2 Materials and methods

2.1 Data collection

Single-cell sequencing datasets (GSE141445) [16] and (GSE181294) [17] were obtained from the Gene Expression Omnibus (GEO) database, which included 31 tumour samples and 20 adjacent normal samples. PCa spatial transcriptomics data (and normal prostate samples were downloaded from the Gene Expression Omnibus (GEO) with number GSE230282 [18] and 10 × Genomics website (https://www.10xgenomics.com/cn/datasets). PCa patients from The Cancer Genome Atlas (TCGA) were obtained using the UCSC Xena browser (https://xenabrowser.net/datapages/).

2.2 scRNA-seq data analysis

Cells were first filtered using the R package Seurat [19] with the following criteria: the number of expressed genes was less than 300 or greater than 5000. Only genes expressed in at least three cells were retained. The data were then normalised and the top 3000 highly variable genes were detected using the FindVariableFeatures function. Next, the dimensionality of the scRNA-seq data was reduced by PCA based on 3000 genes, and 20 principal components were selected for further analysis. In addition, soft k-means clustering was performed using the R package harmony [20] to remove batch effects between samples. Finally, cell clustering was performed using the FindClusters function with a resolution of 0.4. To determine cell types, cells were annotated based on known markers and singleR [21].

2.3 Cellt percentage statistics between groups

To determine the difference in the proportion of different cell types between PCa patients and normal controls, we calculated the proportion of all cell types in each sample and performed between-group significance statistics using Student's t-test.

2.4 Analysis of T cell subtype

The data was normalised and the top 1000 highly variable genes were detected using the FindVariableFeatures function. Next, the dimensionality of the scRNA-seq data was reduced by PCA based on 1000 genes, and 10 principal components were selected for further analysis. In addition, soft k-means clustering was performed using the R package harmony to remove batch effects between samples. Finally, the FindClusters function was used for cell clustering and the resolution was set to 0.4. To determine the cell subtype, we annotated the cells based on known markers and singleR. After completing the annotation of T cell subtypes, the 'FindAllMarkers' function was used to identify the upregulated genes of each subtype with the parameters min.pct = 0.25, logfc.threshold = 0.25, and the 'DoHeatmap' function was used to display the top 10 genes of each cell type. KEGG enrichment analysis was then performed on the differentially expressed genes using the default parameters using the R package clusterProfiler [22]. Based on the ' HALLMARK_OXIDATIVE_PHOSPHORYLATION ' gene set, the AUCell [23] R package was used to score each cell subtype, and t-test was used to statistically analyse the scores of Tregs cells between the PCa patient group and the healthy controls group. The upregulated genes of Tregs cells in different groups using the FindAllMarkers function have the same parameters as described above. Perform a GO biological process enrichment analysis on the differentially expressed genes using the clusterProfiler R package with default parameters. And use the GEPIA2 website [24] to perform survival analysis based on TCGA-PRAD.

2.5 Trajectory analysis of Tregs

To further identify the relationship between the differentiation status of Tregs cells and their hypoxic phenotype, we analysed all Tregs cells using the monocle2 R package [25] and default parameters, and displayed the apoptotic signaling pathwayscore and expression status of key apoptotic signaling pathway genes along the differentiation trajectory. The 'differentialGeneTest' function is used to search for temporally differential genes and divide them into three clusters. Then use the clusterProfiler R package for GO biological process analysis.

2.6 Cell communication analysis

To investigate potential crosstalk between different cells, we used the R package CellChat [26]. We followed a standardised workflow. First, we used the identifiyOverexpressedGenes and identifiyOverexpressedInteractions functions to process the data with standard parameters. The potential ligand-receptor (L/R) interactions in all cells were then calculated and analysed using the computeImmunoProb and computeCommunoProbPathway functions. We focus on the interaction between Tregs cells and other cells.

2.7 Identification of key modules for Tregs

In order to further investigate the key modules mediating the relationship between Tregs cells and immunosuppressive phenotypes, we analyzed the tumors Tregs cells based on sample sources and performed module analysis using the R package hdWGCNA [27] to identify potential modules and genes highly associated with immunosuppression. Use the 'ModulaExprScore' function to calculate the central gene feature scores for each module. Subsequently, the 'ModuleNetworkPlot' function was used to visualize the top 25 core genes of each module, and the clusterProfiler R package for KEGG analysis was used. The 'FindDMEs' function was used to determine the modules with the most significant changes in Tregs of PCa patients.

2.8 Spatial transcriptomics data analysis

The R package Seurat is used to create objects and the SCTransform function is used to standardise the data. The top 3000 highly variable genes were detected using the FindVariableFeatures function, and 30 principal components were selected for further analysis. To eliminate the batch effect between samples, soft K-means clustering was performed using the R package harmony. The FindClusters function was used for clustering and the resolution was set to 0.4. The FindAllMarkers function was used to obtain the marker genes of Tregs cells, with the same parameters as above. Then, based on the different Tregs module genes a, the ST data were scored using the 'AddModulus Score' function, and the differences in module scores between each sample were tested using analysis of variance. For the Visium HD data, analysis was conducted based on a resolution of 16 μm, and the spatial expression patterns of PPIA and BSG were visualised using the 'SpatialFeaturePlot' function. The GEPIA2 website was then used to perform differential statistics on the above ligand/receptor pairs, with a parameter of log2fc. threshold = 0.25 and a P value < 0.05, and to predict their impact on patient survival using default parameters.

2.9 Prediction of prognosis related genes

To determine the potential association between Tregs cell modules with significant changes in PCa patients and patient prognostic risk,, we performed univariate Cox regression analysis on TCGA-PRAD data using M2 module genes and the Survival R package [28, 29] to identify genes significantly associated with patient prognosis, and performed correlation and survival analysis on these genes using the GEPIA2 website.

2.10 Statistical analysis

All statistical analyses in this study were performed using R software version 4.1.3. Student's t-test was used to compare variables between groups. A P value less than 0.05 was considered statistically significant (*P < 0.05, **P < 0.01, ***P < 0.001, ****P < 0.0001).

3 Results

3.1 Single cell multi sample data integration

The GSE141445 dataset contains single cell sequencing data from 13 PCa tissues,and the GSE181294 dataset contains single cell sequencing data for 20 normal prostate tissues and 18 PCa tissues. After quality control measures, 205,337 high quality cells were obtained. After removing the batch effect, all samples were subjected to dimensionality

reduction processing (Fig. 1A). And we identified 9 major cell types (Fig. 1B). The proportions of each cell type varied between samples, reflecting the heterogeneity between patients (Fig. 1C) and the bubble plots show typical markers for each cell type (Fig. 1D). The box plot shows the difference in the proportion of each cell type between different groups (Fig. 1E), and the proportion of T/NK cells decreased significantly in the PCa patient group.

3.2 The intergroup heterogeneity of T cell subtypes

We then annotated T cells into subpopulations and obtained five different cell subtypes (Fig. 2A). Next, the differentially expressed genes of the five T cell subtypes were obtained by differential analysis (Fig. 2B), after which KEGG enrichment analysis was performed, and Tregs cells were significantly enriched in oxidative phosphorylation pathway (Fig. 2C). To further determine the oxidative phosphorylationcharacteristics of different T cell subtypes, we performed oxidative phosphorylationscores and found that Tregs cells exhibited the highest oxidative phosphorylationcharacteristics (Fig. 2D), and the number of Tregs cells in the PCa group significantly increased (Fig. 2E), with oxidative phosphorylation characteristics also significantly higher than those in the control group (Fig. 2F). The TCGA-PRAD and GETx prostate bulk RNA data also showed a significant increase in the proportion of Tregs cells in the tumor group (Fig. 2G). The subsequent differential gene analysis identified the upregulated genes of Tregs cells in

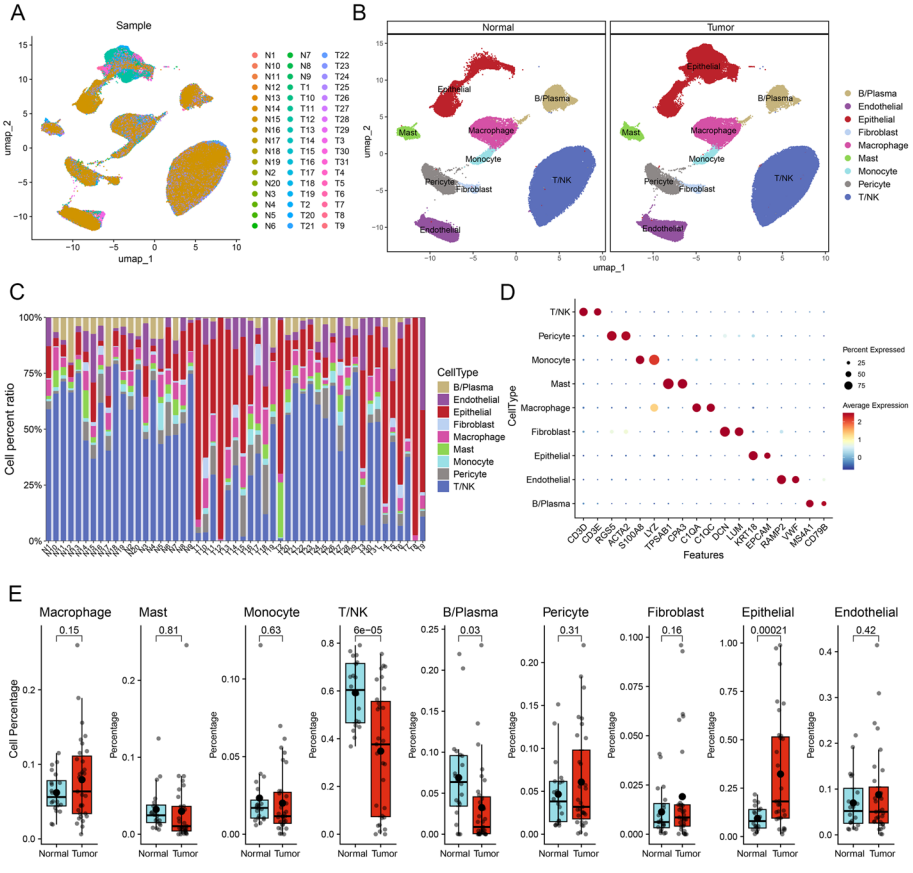

Fig. 1 Single cell multi sample data integration. **A** UMAP of sample size. **B** The umap plot shows the main nine cell types. **C** The bar graph shows the proportion of nine cell types in each sample. **D** Bubble plots show marker genes for each cell type. **E** Boxplots show the difference in the proportion of each cell type in different groups

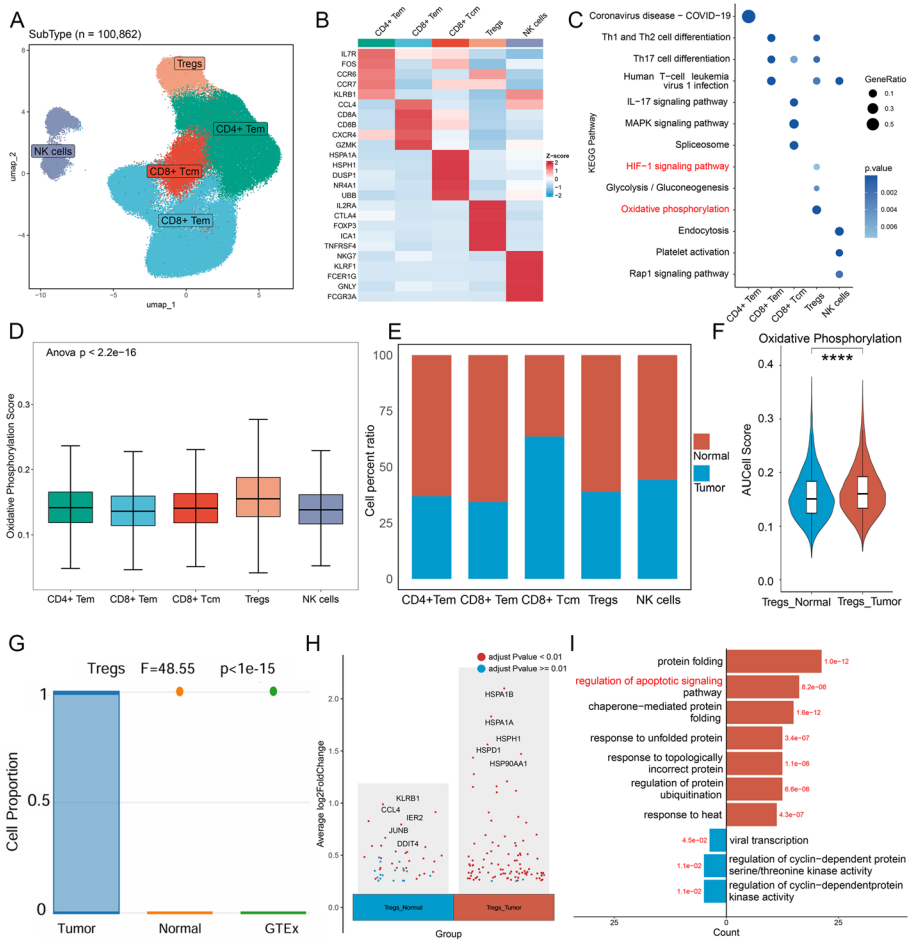

Fig. 2 The intergroup heterogeneity of T cell subtypes. **A** The umap plot shows the five T cell subtypes. **B** The Heatmap shows the top5 marker of each T cell subtype. **C** The bubble plot shows the KEGG enrichment results of each T cell subtype. **D** Boxplots show the differences in scores of different T cell subsets. **E** The bar chart shows the changes in the proportion of cells between groups. **F** Violin plots show the score of Tregs cells in different groups. **G** The bar chart shows the infiltration differences of Tregs in different samples of TCGA-PRAD. (H) The volcano plot shows the upregulated genes of Tregs cells between different groups. **I** Bar graphs show the results of go biological processes in different Tregs cell groups

different groups (Fig. 2H), and the GO biological process enrichment analysis showed that Tregs cells in the tumour group were significantly enriched in regulation of apoptotic signaling pathway (Fig. 2I).

3.3 Tregs cell differentiation trajectory

We further determined the differentiation order of Tregs cells by pseudo time-course analysis (Fig. 3A), and Tregs cells in the control group were at the starting point of differentiation, while Tregs cells in the tumour group were at the end point of differentiation (Fig. 3B). We then identified five differentiation states (Fig. 3C). The apoptotic signaling pathway score increased continuously with the differentiation of the Tregs cells (Fig. 3D). In addition, we observed that gene expression in the apoptotic signaling pathway increased with the differentiation trajectory (Fig. 3E). Moreover, the apoptotic regulatory signaling pathway also showed high activity in State4 (Fig. 3F). Based on pseudo time difference analysis, the expression levels of apoptosis related genes significantly increased in the late stage of development (Fig. 3G). The key genes involved

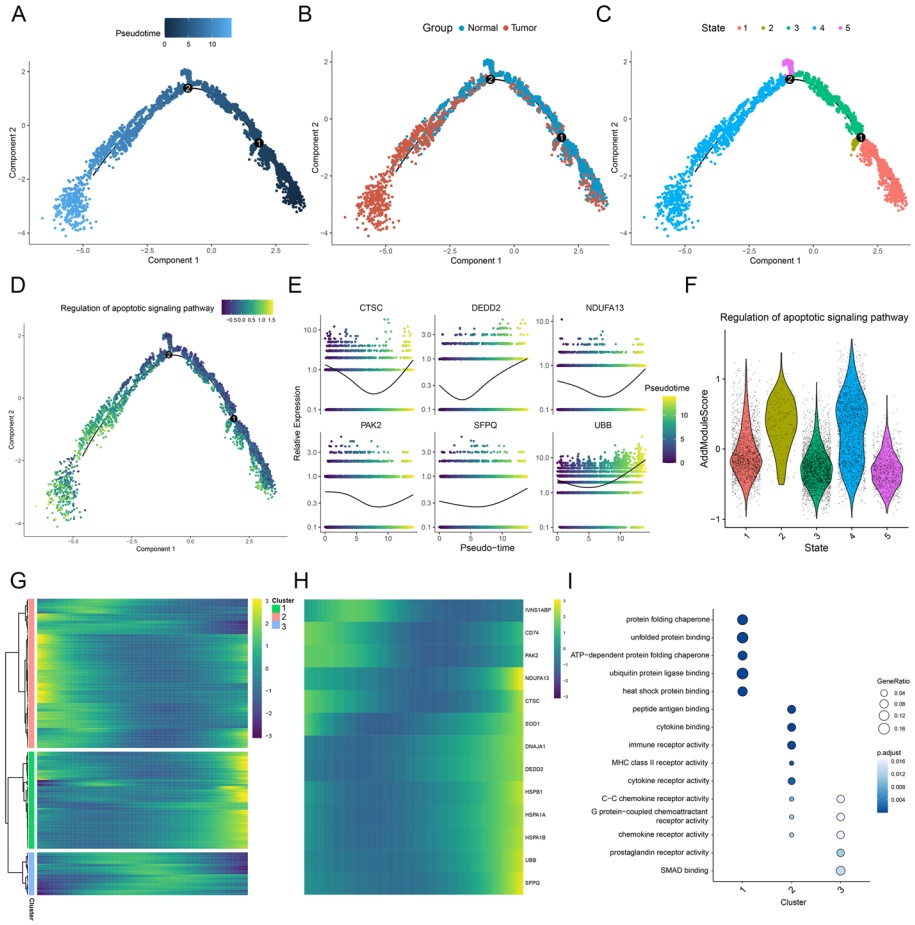

Fig. 3 Tregs cell differentiation trajectory. **A** Differentiation trajectory of Tregs cells. **B** Differentiation order of Tregs cells. **C** The differentiation status of Tregs cells. **D** Trajectory of apoptotic score. **E** Expression of apoptotic related genes with differentiation time. **F** The apoptotic score in different Tregs state. **G** Heatmap showing key genes changing with differentiation time. **H** Pseudo time heatmap of 13 apoptotic pathway genes. **I** GO biological process analysis results of differentiation key genes

in the differentiation process were grouped into three clusters (Fig. 3H), with cluster2 representing early development, cluster3 representing mid development, and cluster1 representing late development. GO biological process functional annotation was then performed on these differentiation clusters, we found that the biological processes involved by Tregs cells at different stages of differentiation showed significant heterogeneity (Fig. 3I). At early stages of differentiation, biological processes related to immune receptor activity are significantly enriched, whereas at late stages of differentiation, biological processes related to ubiquitin protein ligase binding are significantly enriched.

The crosstalk between Tregs and tumor cells We then analysed the interactions between all cells in the normal and tumour groups. The results showed that the number and intensity of intercellular communications were significantly increased in the tumour group compared to the control group (Fig. 4A). The communication network diagram showed that there were significantly more interactions between cells in the tumour group (Fig. 4B). The heat map of the overall pathway level analysis showed that there was more cell communication in the tumour group (Fig. 4C). Subsequent pathway analysis showed a significant increase in the probability of Tregs cells and epithelial cells communicating through the CypA pathway in the tumor group (Fig. 4D). Ligand receptor

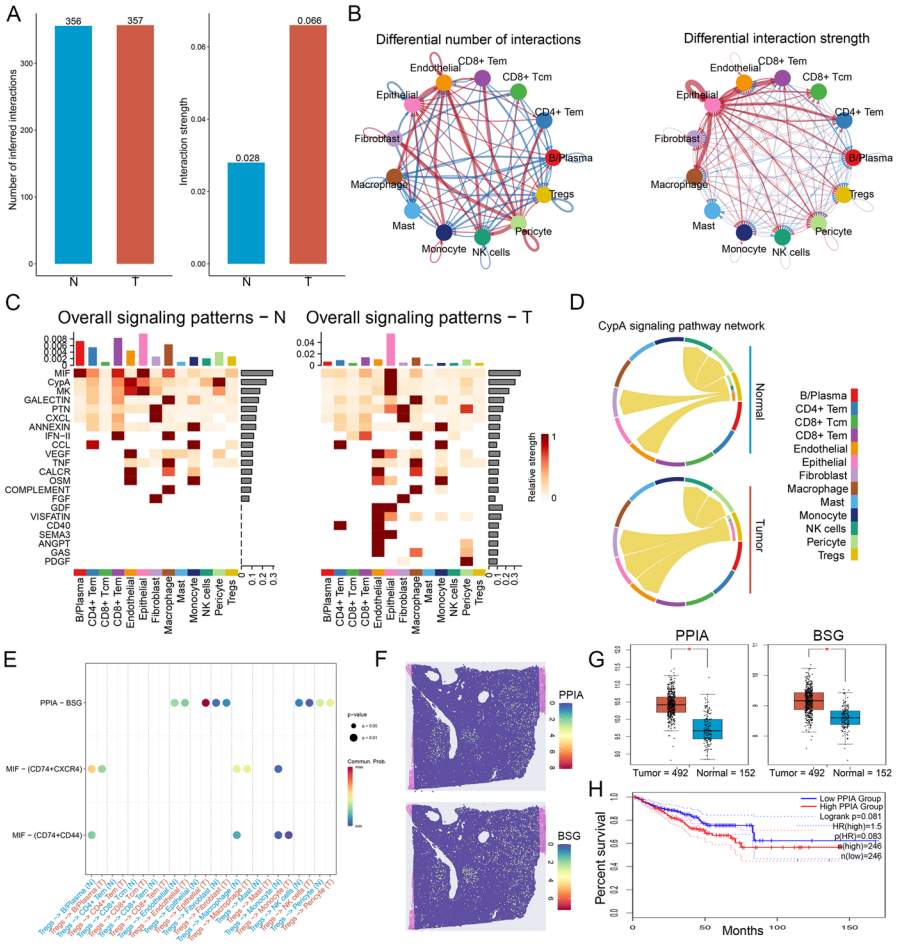

Fig. 4 Epithelial-T cell interactions. **A** The bar graph shows the differences in the number and strength of cell interactions between different groups. **B** The circos plot illustrates the variations in the quantity and intensity of interactions among different cell types across various groups. **C** The heatmap illustrates the signaling patterns of each cell type across different groups. **D** Differences in CypA signaling pathway among different groups. **E** Bubble plot shows the ligand-receptor pairs between stromal cells and immune cells. **F** Spatial expression localization of PPIA-BSG. **G** Box plot shows the expression differencesof PPIA-BSG in different groups of TCGA-PRAD. **H** The KM curve shows the prognostic association of PPIA in TCGA-PRAD

analysis showed that the probability of communication between Tregs cells and epithelial cells via Peptidylprolyl isomerase A (PPIA, ligand)—Basigin (BSG, receptor) was significantly increased in the tumour group (Fig. 4E). In addition, high-resolution spatial transcriptome data analysis revealed significant co-localization signals between PPIA and BSG in PCa tissue (Fig. 4F). To validate this finding, we conducted analysis using the TCGA-PRAD cohort and confirmed that the expression of PPIA and BSG was significantly upregulated in tumor tissues (Fig. 4G). Survival analysis further confirmed that the high expression of PPIA is significantly correlated with poor prognosis in patients (Fig. 4H).

3.4 Identification of key modules driving immune suppression in Tregs

To clarify the key modules involved in the immune suppressive microenvironment in Tregs cells, we first extracted all Tregs cells from PCa patients and obtained 9 cell subpopulations (Fig. 5A). The subsequent high-dimensional weighted gene co-expression

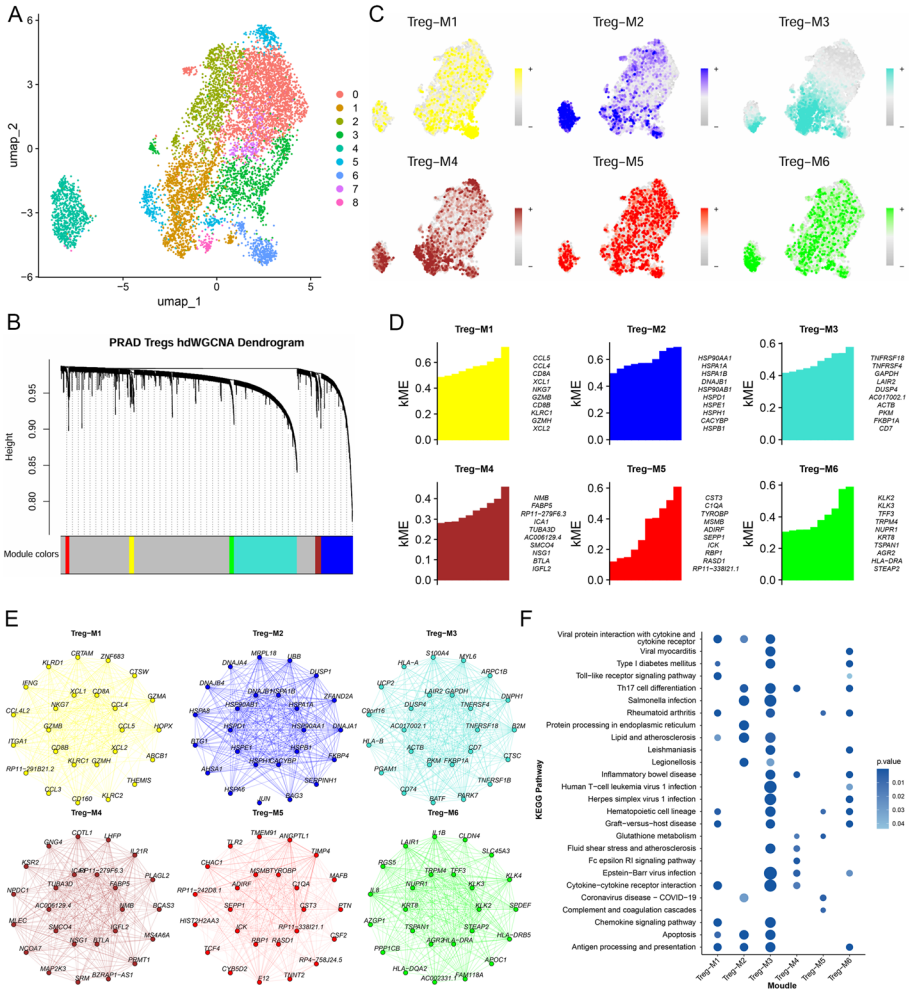

Fig. 5 Identification of key modules driving immune suppression in Tregs. **A** The umap shows the different clustersof all Tregs. **B** Tregs cells are divided into different modules. **C** UAMP diagrams for each Tregs module. **D** Top 10 gene bar charts for each module. **E** The network diagram shows the main modules and key genes. **F** The bubble plot displays the KEGG enrichment analysis results of different module genes

network analysis divided Tregs cells into six different modules (Fig. 5B). The module scores show the distribution of these modules in UMAP, with M2 modules specifically enriched in Cluster4 and M3 modules specifically enriched in Cluster1 (Fig. 5C). Ranked the genes of each module by kME and show the top 10 genes (Fig. 5D), and the Co-expression network analysis revealed the key genes in each module (Fig. 5E). Further KEGG pathway enrichment analysis showed that these Tregs cell modules were significantly enriched in multiple signaling pathways closely related to immune suppression function, revealing their potential mechanisms of action (Fig. 5F). Among them, M2 and M3 modules exhibit synergistic enrichment in the pathways of "antigen processing and presentation" and "cell apoptosis", revealing their mechanisms driving immune suppression from the source of immune recognition to the clearance of effector cells.

3.5 Spatial transcriptomics confirms the localisation of Tregs modules

To further confirm the above findings, we introduced spatial transcriptomic data of PCa and normal prostate samples (Fig. 6A). Based on the gene sets of the aforementioned Treg cell modules, we performed module activity scoring on the ST data and

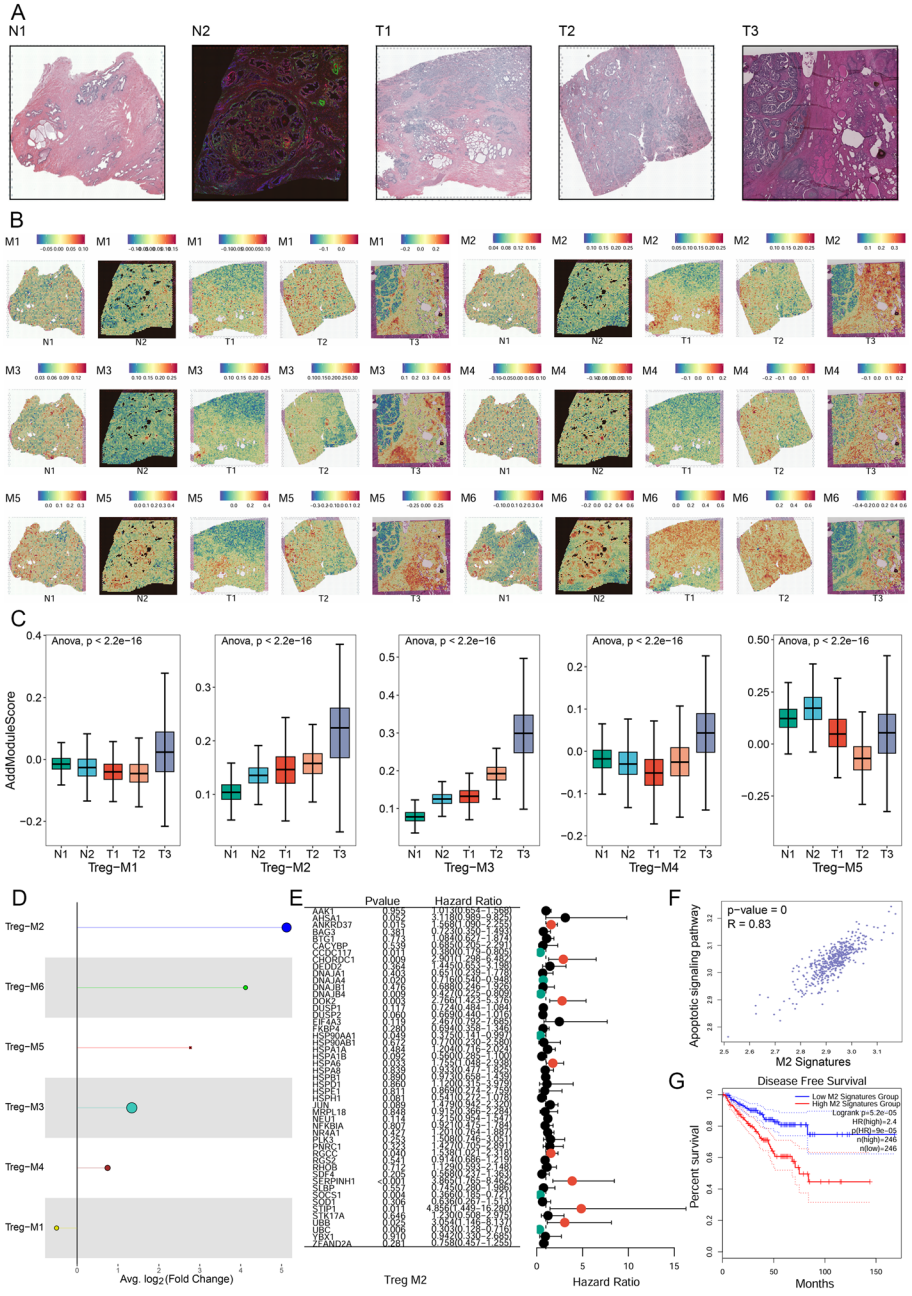

Fig. 6 Spatial transcriptomics confirms the co-localisation of hypoxia and Tregs modules. **A** H&E sections of different prostate samples. **B** Distribution of different Tregs modules in spatial transcriptome data of prostate sample. **C** The box plot of different Tregs modules score in each sample. **D** DEM analysis of different Tregs modules. **E** Multivariate Cox analysis of M2 module genes in TCGA-PRAD. **F** The correlation between apoptosisgene sets and M2 module hub genes in TCGA-PRAD. **G** Survival analysis of M2 module genes in TCGA-PRAD

visualized their spatial distribution, which revealed the spatial organization patterns of these immunosuppressive modules within the tumor tissue (Fig. 6B). Further quantitative analysis of module activity revealed that M2 and M3 scores exhibited a consistent increasing trend across PCa samples (Fig. 6C). Differential module eigengene analysis revealed M2 module as the most significantly upregulated module in the tumor groups (Fig. 6D). To identify prognosis-associated molecules in PCa, we performed multivariate Cox regression analysis on the M2 module genes in TCGA-PRAD data and

identified eight genes—ANKRD37, CHORDC1, DOK2, HSPA6, RGCC, SERPINH1, STIP1, and UBB, that were significantly associated with an increased risk of poor patient outcome(Fig. 6E). Subsequent correlation analysis revealed a strong positive association (r = 0.83) between these molecules and the apoptosis signaling pathway, suggesting their involvement in the synergistic function of immune suppression (Fig. 6F). Consistent with this finding, survival analysis confirmed that their expression was significantly correlated with poorer clinical outcomes (Fig. 6G).

4 Discussion

We used single-cell transcriptomics to determine different modules of Tregs cells in PCa patients, and introduced spatial transcriptomics to analyse the spatial distribution of Tregs modules. The results showed that the M2 module was significantly enriched in the immunosuppressive pathway and exhibited significant inter group differences. Simultaneously, we obtained the core gene set of the M2 module and applied a Cox proportional hazards model to the TCGA-PRAD dataset, leading to the identification of multiple risk factors significantly associated with prognosis, including ANKRD37, CHORDC1, DOK2, HSPA6, RGCC, SERPINH1, STIP1, and UBB. Correlation analysis revealed a strong positive association between these molecules and the apoptosis signaling pathway, disease-free survival analyses confirmed the strong association of these genes with PCa patient outcomes.

Many previous studies have shown that intratumoral immune cell infiltration is the most important predictor of patient survival [5]. Treg cells are one of the most common immunosuppressive cells in tumours, which can suppress anti-tumour immunity and promote cancer progression [30], and the abnormal secretion of PPIA can promote tumor metastasis [31]. We further determined that Trgs cells and malignant cells can form an immunosuppressive microenvironment through PPIA-BSG ligand-receptor pairs. The spatial co-localisation of PPIA-BSG in PCa suggests that their interaction in the tumour microenvironment may have significant implications for tumour development and immune escape. Tregs cells may form a positive feedback mechanism with tumourcells through the PPIA-BSG axis, promoting tumour cell growth and survival. This interaction may lead to immune escape of the tumour, further exacerbating the condition.

Based on these findings, we hypothesise that oxidative phosphorylationconditions within the tumour microenvironment may play an important role in modulating immune responses, particularly through the regulation of Treg (regulatory T cells) activity. Research has shown that unlike other CD4 + T cells, Treg cells primarily rely on mitochondrial oxidative phosphorylation to meet their energy needs and continue to to maintain their immunosuppressive function [32, 33]. The difference in this metabolic characteristic may be the key metabolic basis for shaping the immunosuppressive in the tumor microenvironment. On the one hand, tumor cells consume a large amount of glucose in the microenvironment through anaerobic glycolysis, directly inhibiting the activation and proliferation of effector T cells and anti-tumor immune cells [34]. On the other hand, low oxygen conditions themselves also enhance this advantage by regulating the metabolic signaling pathways of Tregs, further improving their oxidative phosphorylation efficiency and consolidating the immunosuppressive phenotype of Tregs [35]. In addition, Treg can reprogram its own metabolism, including upregulating lactate

metabolism, enhancing FAO, and turning towards OXPHOS, allowing cells to survive and expand in nutrient poor environments [36–38].

Moreover, our findings suggest that four specific risk factors associated with Treg cells (ANKRD37, CHORDC1, DOK2, HSPA6, RGCC, SERPINH1, STIP1, and UBB) may serve as molecular signatures for poor prognosis in PCa patients. These factors may reflect the dynamic interaction between the tumor cells, the immune cells, and the surrounding microenvironment, providing valuable insights into the mechanisms driving immune evasion and tumor progression. Therefore, these risk factors could potentially be used as clinical diagnostic tools for identifying high-risk PCa patients, as well as prognostic biomarkers to predict treatment outcomes. Notably, these genes exhibit a strong positive correlation with the activity of the apoptotic signaling pathway in the TCGA-PRAD dataset, implying a close regulatory link between them. The apoptotic signaling pathway, beyond its canonical role in inducing cell death, plays a non-negligible part in shaping the immunosuppressive tumor microenvironment. On one hand, the accumulation of apoptotic tumor cells or immune cells releases a large number of damage-associated molecular patterns, which can recruit myeloid-derived suppressor cells and tumor-associated macrophages to the tumor site, further amplifying the immune-suppressive milieu [39–41]. On the other hand, activated apoptotic signaling can directly impair the function of effector T cells—for instance, by upregulating the expression of programmed death ligand 1 (PD-L1) on tumor cells, it induces the exhaustion of cytotoxic T lymphocytes, thereby weakening the anti-tumor immune response [42, 43].

There are several limitations to this study. First, there is a lack of validation of clinical patient-related information. Second, the study was only validated from a multi-omics perspective and specific molecular validation efforts were lacking. Thirdly, the data analysis was only based on bioinformatics methods, which require further validation by in vivo and in vitro experiments.Third, given the atypical pathological features of our samples, we recommend that future studies validate these findings in a pure adenocarcinoma cohort. Finally, the specific mechanisms of Tregs cells in the tumour microenvironment need to be further investigated.

In conclusion, targeting Tregs, particularly by inhibiting the PPIA-BSG pathway, is a promising avenue for the development of new cancer immunotherapies. By interfering with the immunosuppressive role of Tregs, it may be possible to enhance the anti-tumour immune response and thereby improve the prognosis and outcome of PCa patients. In addition, investigating the molecular mechanisms by which hypoxia drives Treg function may provide further opportunities to identify novel therapeutic targets and improve the overall efficacy of cancer immunotherapy. As such, this area of research holds great potential for advancing our understanding of cancer immunology and developing more effective treatment strategies for PCa and other solid tumours.

Acknowledgements
Not applicable.

Author contributions
Zongwei Mei and Chen Chen performed the data; Zongwei Mei contributed significantly to analysis and manuscript preparation; Zongwei Mei performed the data analyses and wrote the manuscript; Jilong Zhou and Qing Jiang contributed to the conception of the study; Zongwei Mei and Qing Jiang helped perform the analysis with constructive discussions.

Funding
Not applicable.

Data availability
The datasets analyzed in this study are publicly available in the Gene Expression Omnibus (GEO) repository under accession numbers GSE141445, GSE181294, and GSE230282; from the 10×Genomics website (https://www.10xgenomics.com/cn/datasets); and from The Cancer Genome Atlas (TCGA) via the UCSC Xena browser (https://xenabrowser.net/datapages/).

Declarations

Ethics approval and consent to participate
Not applicable.

Consent for publication
Not applicable.

Informed consent
Not applicable.

Competing interests
The authors declare no competing interests.

Received: 24 January 2025 / Accepted: 6 January 2026
Published online: 23 February 2026

References

1. Chan JM, Zaidi S, Love JR, Zhao JL, Setty M, Wadosky KM, et al. Lineage plasticity in prostate cancer depends on JAK/STAT inflammatory signaling. Science. 2022;377(6611):1180–91.
2. Bian X, Wang W, Abudurexiti M, Zhang X, Ma W, Shi G, et al. Integration analysis of single-cell multi-omics reveals prostate cancer heterogeneity. Adv Sci. 2024;11(18):e2305724.
3. Binnewies M, Roberts EW, Kersten K, Chan V, Fearon DF, Merad M, et al. Understanding the tumor immune microenvironment (TIME) for effective therapy. Nat Med. 2018;24(5):541–50.
4. Ali HR, Chlon L, Pharoah PD, Markowetz F, Caldas C. Patterns of immune infiltration in breast cancer and their clinical implications: a gene-expression-based retrospective study. PLoS Med. 2016;13(12):e1002194.
5. Bindea G, Mlecnik B, Tosolini M, Kirilovsky A, Waldner M, Obenauf AC, et al. Spatiotemporal dynamics of intratumoral immune cells reveal the immune landscape in human cancer. Immunity. 2013;39(4):782–95.
6. Mlecnik B, Bindea G, Angell HK, Maby P, Angelova M, Tougeron D, et al. Integrative analyses of colorectal cancer show immunoscore is a stronger predictor of patient survival than microsatellite instability. Immunity. 2016;44(3):698–711.
7. Sautès-Fridman C, Lawand M, Giraldo NA, Kaplon H, Germain C, Fridman WH, et al. Tertiary lymphoid structures in cancers: prognostic value, regulation, and manipulation for therapeutic intervention. Front Immunol. 2016;3(7):407.
8. Osman A, Yan B, Li Y, Pavelko KD, Quandt J, Saadalla A, et al. TCF-1 controls T(reg) cell functions that regulate inflammation, CD8(+) T cell cytotoxicity and severity of colon cancer. Nat Immunol. 2021;22(9):1152–62.
9. Quezada SA, Peggs KS, Simpson TR, Allison JP. Shifting the equilibrium in cancer immunoediting: from tumor tolerance to eradication. Immunol Rev. 2011;241:104–18.
10. Roychoudhuri R, Eil RL, Restifo NP. The interplay of effector and regulatory T cells in cancer. Curr Opin Immunol. 2015;33:101–11.
11. Saleh R, Elkord E. FoxP3 T regulatory cells in cancer: prognostic biomarkers and therapeutic targets. Cancer Lett. 2020;490:174–85.
12. Stenstrom J, Hedenfalk I, Hagerling C. Regulatory T lymphocyte infiltration in metastatic breast cancer-an independent prognostic factor that changes with tumor progression. Breast Cancer Res. 2021;23:27.
13. Soo RA, et al. Prognostic significance of immune cells in non-small cell lung cancer: meta-analysis. Oncotarget. 2018;9:24801–20.
14. De Simone M, Arrigoni A, Rossetti G, Gruarin P, Ranzani V, Politano C, et al. Transcriptional Landscape of Human Tissue Lymphocytes Unveils Uniqueness of Tumor-Infiltrating T Regulatory Cells. Immunity. 2016;45(5):1135–47.
15. Pan Y, Zhou H, Sun Z, Zhu Y, Zhang Z, Han J, et al. Regulatory T cells in solid tumor immunotherapy: effect, mechanism and clinical application. Cell Death Dis. 2025;16(1):277. https://doi.org/10.1038/s41419-025-07544-w.
16. Chen S, Zhu G, Yang Y, Wang F, Xiao YT, Zhang N, et al. Single-cell analysis reveals transcriptomic remodellings in distinct cell types that contribute to human prostate cancer progression. Nat Cell Biol. 2021;23(1):87–98.
17. Hirz T, Mei S, Sarkar H, Kfoury Y, Wu S, Verhoeven BM, et al. Dissecting the immune suppressive human prostate tumor microenvironment via integrated single-cell and spatial transcriptomic analyses. Nat Commun. 2023;14(1):663.
18. Watanabe R, Miura N, Kurata M, Kitazawa R, Kikugawa T, Saika T. Spatial gene expression analysis reveals characteristic gene expression patterns of de novo neuroendocrine prostate cancer coexisting with androgen receptor pathway prostate cancer. Int J Mol Sci. 2023;24(10):8955.
19. Hao Y, Hao S, Andersen-Nissen E, Mauck WM 3rd, Zheng S, Butler A, et al. Integrated analysis of multimodal single-cell data. Cell. 2021;184(13):3573-3587.e29.
20. Korsunsky I, Millard N, Fan J, Slowikowski K, Zhang F, Wei K, et al. Fast, sensitive and accurate integration of single-cell data with Harmony. Nat Methods. 2019;16(12):1289–96.
21. Aran D, Looney AP, Liu L, Wu E, Fong V, Hsu A, et al. Reference-based analysis of lung single-cell sequencing reveals a transitional profibrotic macrophage. Nat Immunol. 2019;20(2):163–72.
22. Wu T, Hu E, Xu S, Chen M, Guo P, Dai Z, et al. clusterProfiler 40: A universal enrichment tool for interpreting omics data. Innovation (Camb). 2021;2(3):100141.

23. Aibar S, González-Blas CB, Moerman T, Huynh-Thu VA, Imrichova H, Hulselmans G, et al. SCENIC: single-cell regulatory network inference and clustering. Nat Methods. 2017;14(11):1083–6.
24. Tang Z, Kang B, Li C, Chen T, Zhang Z. GEPIA2: an enhanced web server for large-scale expression profiling and interactive analysis. Nucleic Acids Res. 2019;47(W1):W556–60.
25. Qiu X, Hill A, Packer J, Lin D, Ma YA, Trapnell C. Single-cell mrna quantification and differential analysis with census. Nat Methods. 2017;14(3):309–15.
26. Jin S, Guerrero-Juarez CF, Zhang L, Chang I, Ramos R, Kuan CH, et al. Inference and analysis of cell-cell communication using Cell Chat. Nat Commun. 2021;12(1):1088.
27. Morabito S, Reese F, Rahimzadeh N, Miyoshi E, Swarup V. hdWGCNA identifies co-expression networks in high-dimensional transcriptomics data. Cell Rep Methods. 2023;3(6):100498.
28. Xun Z, Zhou H, Shen M, Liu Y, Sun C, Du Y, et al. Identification of hypoxia-ALCAM(high) macrophage- exhausted T cell axis in tumor microenvironment remodeling for immunotherapy resistance. Adv Sci (Weinh). 2024;11(33):e2309885.
29. Tan QH, Harmston N, Tolwinski NS. ggbulksurv: An R package for easy Drosophila and C. elegans survival analysis. MicroPubl Biol. 2024. https://doi.org/10.17912/micropub.biology.001060.
30. Shitara K, Nishikawa H. Regulatory T cells: a potential target in cancer immunotherapy. Ann N Y Acad Sci. 2018;1417(1):104–15.
31. Wang X, Qu Y, Xu Q, Jiang Z, Wang H, Lin B, et al. NQO1 triggers neutrophil recruitment and NET formation to drive lung metastasis of invasive breast cancer. Cancer Res. 2024;84(21):3538–55. https://doi.org/10.1158/0008-5472.CAN-24-0291.
32. Jiang Z, Wang H, Wang X, Duo H, Tao Y, Li J, et al. TMED4 facilitates regulatory T cell suppressive function via ROS homeostasis in tumor and autoimmune mouse models. J Clin Invest. 2024;135:e179874.
33. Wang Y, Huang T, Gu J, Lu L. Targeting the metabolism of tumor-infiltrating regulatory T cells. Trends Immunol. 2023;44(8):598–612. https://doi.org/10.1016/j.it.2023.06.001.
34. Gu J, Zhou J, Chen Q, Xu X, Gao J, Li X, et al. Tumor metabolite lactate promotes tumorigenesis by modulating MOESIN lactylation and enhancing TGF-β signaling in regulatory T cells. Cell Rep. 2022;39(12):110986. https://doi.org/10.1016/j.celrep.2022.110986.
35. Gao H, Nepovimova E, Heger Z, Valko M, Wu Q, Kuca K, et al. Role of hypoxia in cellular senescence. Pharmacol Res. 2023;194:106841. https://doi.org/10.1016/j.phrs.2023.106841.
36. Raud B, Roy DG, Divakaruni AS, Tarasenko TN, Franke R, Ma EH, et al. Etomoxir actions on regulatory and memory T cells are independent of Cpt1a-mediated fatty acid oxidation. Cell Metab. 2018;28(3):504-515.e7. https://doi.org/10.1016/j.cmet.2018.06.002.
37. Timilshina M, You Z, Lacher SM, Acharya S, Jiang L, Kang Y, et al. Activation of Mevalonate Pathway via LKB1 is essential for stability of Treg Cells. Cell Rep. 2019;27(10):2948-2961.e7. https://doi.org/10.1016/j.celrep.2019.05.020.
38. Michalek RD, Gerriets VA, Jacobs SR, Macintyre AN, MacIver NJ, Mason EF, et al. Cutting edge: distinct glycolytic and lipid oxidative metabolic programs are essential for effector and regulatory CD4+ T cell subsets. J Immunol. 2011;186(6):3299–303. https://doi.org/10.4049/jimmunol.1003613.
39. Tan Y-T, Li T, Wang R-B, Liu Z-K, Ma M-Y, Huang R-Z, et al. WTAP weakens oxaliplatin chemosensitivity of colorectal cancer by preventing PANoptosis. Cancer Lett. 2024;604:217254.
40. Zhang Z, Zhang F, Pang P, Li Y, Chen X, Sun S, et al. Identification of PANoptosis-relevant subgroups to evaluate the prognosis and immune landscape of patients with liver hepatocellular carcinoma. Front Cell Dev Biol. 2023;11:1210456.
41. Wang X, Sun R, Chan S, Meng L, Xu Y, Zuo X, et al. PANoptosis-based molecular clustering and prognostic signature predicts patient survival and immune landscape in colon cancer. Front Genet. 2022;13:955355.
42. Seifert L, Werba G, Tiwari S, Giao Ly NN, Alothman S, Alqunaibit D, et al. The necrosome promotes pancreatic oncogenesis via CXCL1 and Mincle-induced immune suppression. Nature. 2016;532:245–9.
43. Yang Y, Wu M, Cao D, Yang C, Jin J, Wu L, et al. ZBP1-MLKL necroptotic signaling potentiates radiation-induced antitumor immunity via intratumoral STING pathway activation. Sci Adv. 2021;7:eabf6290.

Publisher's Note